Novel Cu labeled RGD-BBN heterotrimers for PET imaging of prostate cancer

Ermelinda Lucente, Hongguang Liu, Yang Liu, Xiang Hu, Enza Lacivita, Marcello Leopoldo, and Zhen Cheng

Bioconjugate Chem., **Just Accepted Manuscript** • DOI: 10.1021/acs.bioconjchem.8b00113 • Publication Date (Web): 27 Mar 2018

Novel ^{64}Cu labeled RGD$_2$-BBN heterotrimers for PET imaging of prostate cancer

Ermelinda Lucente[§#‡], Hongguang Liu[§], Yang Liu[§], Xiang Hu[§], Enza Lacivita[#], Marcello Leopoldo[#*], Zhen Cheng[§*]

[§] Molecular Imaging Program at Stanford (MIPS), Department of Radiology and Bio-X Program, Stanford University, Stanford, California, 94305-5344 [#] Dipartimento di Farmacia-Scienze del Farmaco, Università degli Studi di Bari Aldo Moro, via Orabona, 4, 70125, Bari, Italy [‡] Present Address: FARMALABOR SRL Stabilimento via Pozzillo, zona ind. - 76012 Canosa di Puglia (BT) – Italy

Journal: Bioconjugate Chemistry

Running Title: ^{64}Cu-RGD$_2$-PG$_{12}$-BBN for PET Imaging of Prostate Cancer

[*] Author to whom correspondence should be addressed

ABSTRACT

Bombesin receptor 2 (BB_2) and integrin $\alpha_v\beta_3$ receptor are privileged targets for molecular imaging of cancer because their overexpression in a number of tumor tissues. The most recent developments in heterodimer-based radiopharmaceuticals concern BB_2- and integrin $\alpha_v\beta_3$-targeting compounds, consisting of bombesin (BBN) and cyclic arginine-glycine-aspartic acid peptides (RGD), connected through short length linkers. Molecular imaging probes based on RGD-BBN heterodimer design exhibit improved tumor targeting efficacy compared to the single-receptor targeting peptide monomers. However, their application in clinical study is restricted because of inefficient synthesis or unfavorable in vivo properties, which could depend on the short linker nature. Thus, the aim of the present study was to develop a RGD_2-BBN heterotrimer, composed of (7-14)BBN-NH_2 peptide (BBN) linked to the E[*c*(RGDyK)]$_2$ dimer peptide (RGD_2), bearing the new linker type [Pro-Gly]$_{12}$. The heterodimer E[c(RGDyK)]$_2$-PEG_3-Glu-(Pro-Gly)$_{12}$-BBN(7-14)-NH_2 (RGD_2-PG_{12}-BBN) was prepared through conventional solid phase synthesis, then conjugated with 1,4,7,10-tetraazacyclododecane-1,4,7,10-tetraacetic acid (DOTA) or 1,4,7-triazacyclononane-1-glutaric acid-4,7-diacetic acid (NODA-GA). In ^{64}Cu labeling, the NODA-GA chelator showed superior radiochemical characteristics compared to DOTA (70% *vs.* 40% yield, respectively). Both conjugates displayed dual targeting ability, showing good $\alpha_v\beta_3$ affinities and high BB_2 receptor affinities which, in the case of the NODA-GA conjugate, was in the same range as the best RGD-BBN heterodimer ligands reported to date (Ki= 24 nM). ^{64}Cu-DOTA and ^{64}Cu-NODA-GA probes were also found to be stable after 1 h incubation in mouse serum (> 90%). In a microPET study in prostate cancer PC-3 xenograft mice, both probes showed low tumor

uptake, probably due to poor pharmacokinetic properties *in vivo*. Overall, our study demonstrates that novel RGD-BBN heterodimer with long linker can be prepared and they preserve high binding affinities to BB_2 and integrin $\alpha_v\beta_3$ receptor binding ability. The present study represents a step forward the design of effective heterodimer or heterotrimer probes for dual targeting.

Keywords: BBN; RGD_2; RGD-BBN heterodimer; PET; Prostate Cancer

INTRODUCTION

Interesting developments in design of new cancer targeting pharmaceutical or molecular probe entities involve the synthesis of "bivalent constructs", consisting in two different receptor-targeting peptide ligands which are covalently linked to form heterodimers.[1] This type of approach is called "dual targeting", since the ligand is composed by two moieties that can bind two different biomarkers expressed by tumor cells (heterobivalent interactions), inducing enhanced targeting ability and specificities relative to monovalent binding. Because of the increased number of receptors available for targeting, local ligand concentration or binding kinetics, molecular imaging probes based on these peptide heterodimers could exhibit improved tumor targeting efficacy compared to the single receptor targeting peptide monomers.[2,3]

Recently, a class of peptide heterodimers-based molecular probes for dual targeting of gastrin-releasing peptide (GRP) receptor (GRPR, also known as BB_2 receptor) and integrin $\alpha_v\beta_3$ have been successfully developed.[2-12] BB_2 receptor, which belongs to the bombesin (BBN) G-protein coupled receptors family, has been found to be overexpressed in several types of human cancers, such as lung, colon, gastric, pancreatic, breast and prostate cancers.[13-18] Several BBN peptidic analogs have been labeled with various radioisotopes, such as ^{64}Cu, ^{18}F and ^{68}Ga, for diagnosis of BB_2-positive prostate lesions through PET imaging.[4,19,20] Integrins represent a family of membrane adhesion receptors, that play an essential role in cancer progression. In particular, integrin $\alpha_v\beta_3$ stimulate endothelial cells to give angiogenesis and also induce tumor cell invasion and movement across blood vessels to form metastasis.[21-24] To date, most of the integrin $\alpha_v\beta_3$ targeted PET probes have been developed on the radiolabeling

of arginine-glycine-aspartic acid (RGD) sequence containing antagonists.[25-30] Since prostate cancer expresses both BB_2 and integrin $\alpha_v\beta_3$ receptors, RGD containing cyclic peptide and BBN(7-14) sequence have been connected through short length linkers and radiolabeled with several radionuclides for imaging and therapy.[6-12,31-32] It was discovered that RGD-BBN heterodimers probes displayed increased tumor uptake and tumor-to-nontumor (T/N) ratios, due to the lower liver and non specific tissues accumulation, highlighting the advantages of using the dual targeting approach for cancer molecular imaging.[3-10]

However, disadvantages mainly related to the nature and length of the linker became apparent. The first generation of RGD-BBN heterodimers involved the use of an asymmetric glutamate-based linker, which lead to a mixture of two isomers that significantly hampered the usability of the probe. Other short length linkers developed for RGD-BBN suffers from high costs, difficult and time-consuming synthetic procedures.[3-10] More importantly, the use of a short linker could not allow the heterodimer to bind at the two targets simultaneously, because these two targets could be quite far away from each other spatially. The linker should allow the two peptides to favorably interact with their target receptors. Consequently, the linker should display a good compromise between minimal entropic penalty and high flexibility, also maintaining good physicochemical and pharmacokinetic properties (e.g. high solubility, metabolic stability, low lipophilicity and non-specific binding) and low toxicity.[33] Optimized linker length and hydrophilicity, in $\alpha_v\beta_3$/BB_2-targeted probes, could result in increased tumor to background ratios (Fig. 1).

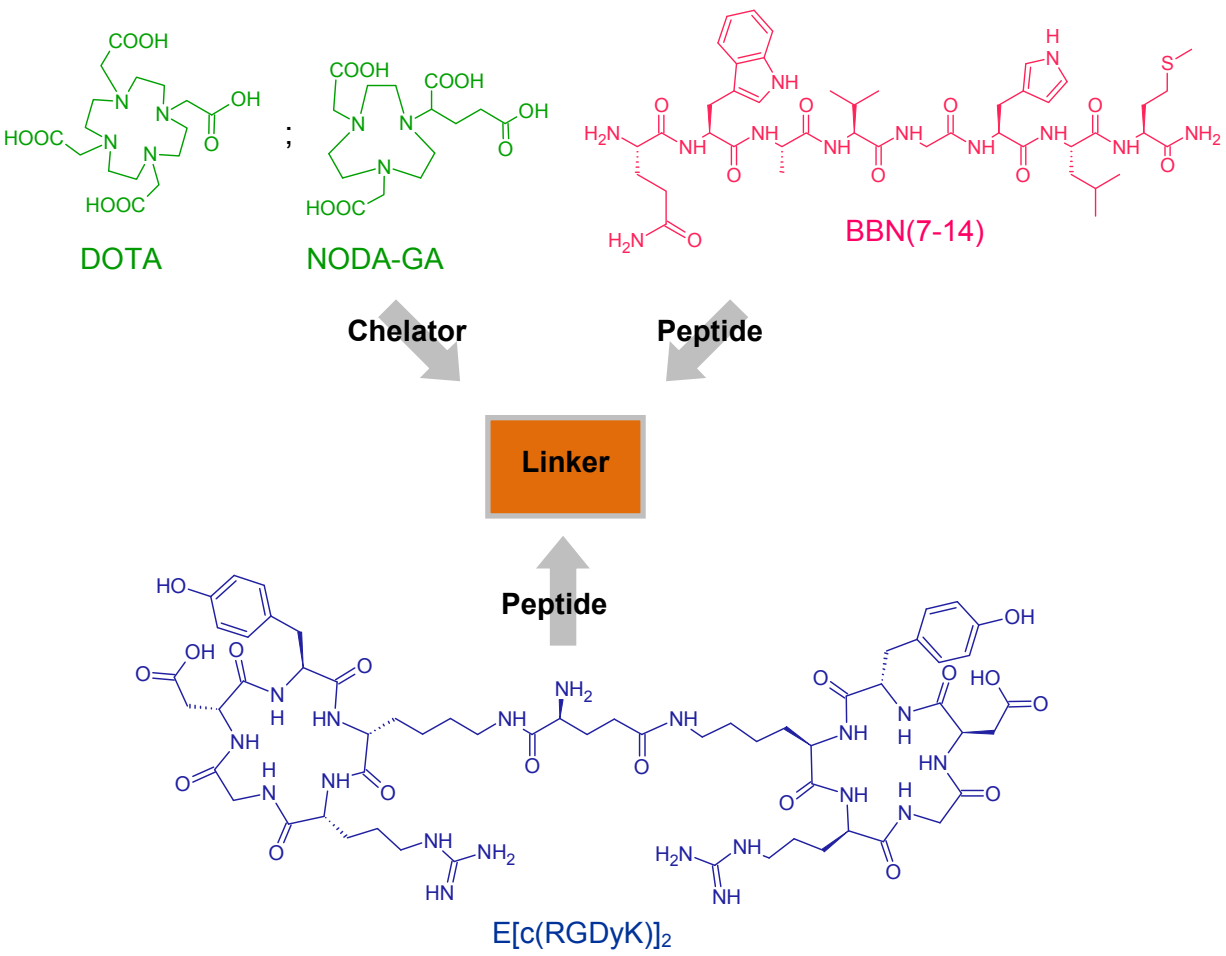

Figure 1. The linker allows the conjugation between the two peptidic ligands and the chelating group.

Therefore, the aim of this study was the development of a RGD-BBN radiotracer with a new type of linker, in order to simplify the probe synthesis, increase the tumor uptake and improve the pharmacokinetic profile. It was hypothesized that a "long chain linker" could display better tumor-targeting efficacy, allowing the two moieties to easily reach the targets exposed on the cell membrane. Furthermore, a "peptidic chain linker" synthesis, using a completely automatized solid phase synthetic procedure, should be much more accessible.

A study of Vagner et al. has reported heterobivalent ligands containing the MSH(7) and Delt-II binding moieties connected through [Pro-Gly]x linkers of different length. These linkers displayed, in their low-energy conformations, a predominant helical structure which is stretchable, thus capable to adapt the correct distance between the two targets.[33] This type of linker fits well into a modular solid-phase synthesis scheme, wherein ligand and linker elements (amino acids) are added systematically. In that study, the heterodimer with $[Pro\text{-}Gly]_{12}$ and $[Pro\text{-}Gly]_{15}$ linkers displayed the highest binding enhancement, compared to $[Pro\text{-}Gly]_3$ and $[Pro\text{-}Gly]_6$ linkers, so the affinity enhancement increased significantly with increasing linker length.[33] On such basis, we selected a $[Pro\text{-}Gly]_{12}$ (PG_{12}) spacer as long chain peptidic linker to design a RGD-BBN conjugate. The probe was designed as heterotrimer (RGD_2-BBN), because E[*c*(RGDyK)]$_2$ dimer (RGD_2) displayed better *in vivo* kinetics than *c*(RGDyK) monomer (RGD), resulting in higher T/N ratio.[25]

This study describes the synthesis, radiosynthesis, *in vitro* and *in vivo* biological evaluation of a new "peptidic long linker" heterotrimeric probes, consisting of RGD_2 and BBN(7-14) moieties, connected together through a PEG_3-Glu-$(Pro\text{-}Gly)_{12}$ linker, (RGD_2-PG_{12}-BBN heterotrimer) and conjugated with DOTA or NODA-GA chelating groups, for ^{64}Cu radiolabeling (Fig. 2).

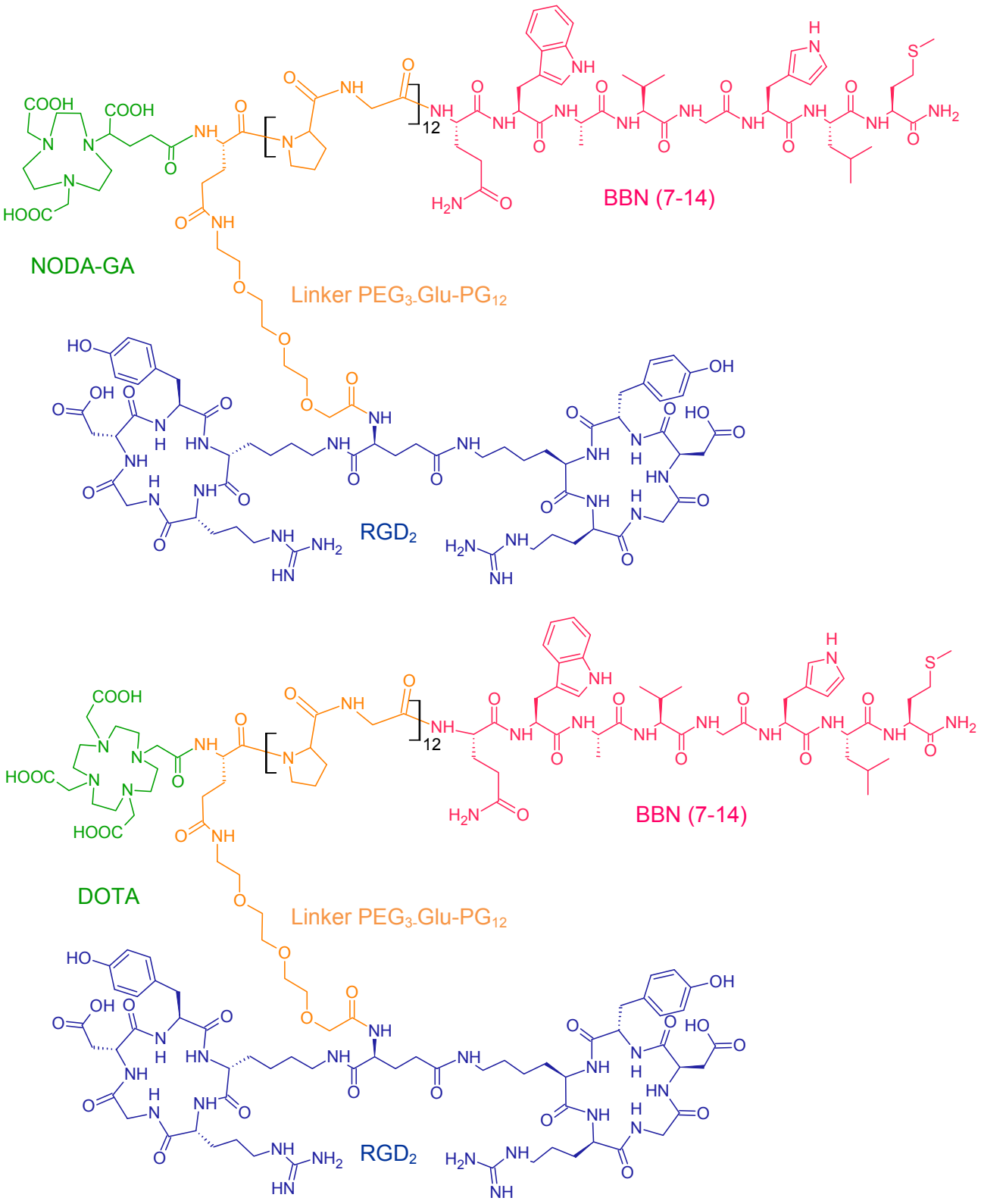

Figure 2. ^{64}Cu-NODA-GA-RGD$_2$-PG$_{12}$-BBN and ^{64}Cu-DOTA-RGD$_2$-PG$_{12}$-BBN chemical structure, with different components.

RESULTS

Chemistry and Radiochemistry

Synthesis and partial deprotection of E-PG_{12}-BBN peptide, achieved by using the conventional Fmoc solid phase peptide synthesis, was carried out with a good yield in 5 days. The peptide was then Boc-protected on N-terminus to prevent the dimerization during the next step. The Boc protection reaction was optimized using different conditions for DMAP catalysis, basic conditions (Et3N, DIPEA, NaOH), and solvent nature (MeCN, MeCN/H_2O, H_2O/THF, DMF). Then, the Boc-E-PG_{12}-BBN peptide was conjugated with RGD_2-PEG_3, by previous activation (2 h) of the glutamic acid side chain with HATU in DMF and DIPEA. Other coupling reagents such as TSTU/DIPEA or EDC/SNHS/DIPEA did not afford the Boc-protected RGD_2-PG_{12}-BBN heterotrimer. After Boc-deprotection, the last step was the heterotrimer conjugation with DOTA and NODA-GA, activated with N-hydroxysuccinimide group (NHS), in DMF and DIPEA. The activation *in situ* of DOTA or NOTA with EDC/SNHS in sodium acetate buffer or H_2O, HATU/DIPEA in DMF or DMSO, TSTU/DIPEA in DMF, PyBOP/DIPEA with or without HOBt in DMF, PyBroP/DIPEA in DMF did not afford the DOTA and NODA-GA conjugates (Fig. 3).

The DOTA-RGD_2-PG_{12}-BBN and NODA-GA-RGD_2-PG_{12}-BBN heterotrimers were successfully labeled with ^{64}Cu; ^{64}Cu-NODA-GA- heterotrimer displayed better ability to be radiolabeled (70% yield) than ^{64}Cu-DOTA-heterotrimer (40% yield). The purification of radioligand solutions afforded ^{64}Cu-DOTA-RGD_2-PG_{12}-BBN or ^{64}Cu-NODA-GA-RGD_2-PG_{12}-BBN with > 95% radiochemical purity, and the specific activity

of the probes was generally about 1.7-4.5 GBq/μmol. From HPLC analysis (Fig. S1), the probes displayed the same retention time (21.1 min) in HPLC analysis.

Mouse Serum Stability

Serum stability studies showed that ^{64}Cu-DOTA-RGD$_2$-PG$_{12}$-BBN and ^{64}Cu-NODA-GA-RGD$_2$-PG$_{12}$-BBN were resistant to proteolysis and transchelation, with > 90% of the probe intact after 1 h incubation in mouse serum at 37 °C.

***In vitro* Cell Assays**

Competitive cell-binding assay was used to determine the BB$_2$ and $\alpha_v\beta_3$ receptors binding affinity of DOTA- and NODA-GA-RGD$_2$-PG$_{12}$-BBN. Both compounds inhibited the binding of ^{125}I-[Tyr^4]BBN to PC-3 cells and ^{125}I-echistatin to U87MG cells in a concentration dependent manner. The results were plotted in sigmoid curves for the IC$_{50}$ values calculation (Table 1).

	IC$_{50}$ PC-3 cells (GRPR) nM	**IC$_{50}$ U87MG cells ($\alpha_v\beta_3$) nM**
DOTA-RGD$_2$-PG$_{12}$-BBN	100.4 ± 73.2	101.2 ± 57.4
NODA-GA-RGD$_2$-PG$_{12}$-BBN	24.3 ± 10.9	165.3 ± 105.4
BBN	1.36	/
RGD$_2$	/	66.6

Table 1. DOTA-RGD$_2$-PG$_{12}$-BBN, NODA-GA-RGD$_2$-PG$_{12}$-BBN, BBN and RGD$_2$ binding affinity results.

***In vivo* Imaging**

PET imaging studies were conducted as follows: in the first experiment mice (n = 4 for each probe) were injected with ^{64}Cu-DOTA- or ^{64}Cu-NODA-GA-RGD$_2$-PG$_{12}$-BBN to compare their imaging ability to detect efficiently the tumor; in the second experiment mice were treated only with ^{64}Cu-NODA-GA-RGD$_2$-PG$_{12}$-BBN, in the presence or absence of saturating doses of BBN and/or RGD$_2$ as blocking agents (n = 3 for each group). PET scans were acquired at 30 min and 1 h after injection and biodistribution studies were performed only on mice injected with ^{64}Cu-NODA-GA conjugate, after 1 h images acquisition.

1) Decay-corrected coronal microPET images are shown in Fig. 3. The PC-3 tumor was clearly visible up to 1 h p.i. with a good tumor-to-background contrast; however, high radioactivity accumulation in the kidney was observed. From a quantification analysis of PET images (Table 2), the tumor uptake of ^{64}Cu-NODA-GA-RGD$_2$-PG$_{12}$-BBN (2.02 ± 0.18 %ID/g 30 min p.i., 1.80 ± 0.34 %ID/g 1 h p.i.) was similar to that of ^{64}Cu-DOTA-RGD$_2$-PG$_{12}$-BBN (1.92 ± 0.24 %ID/g 30 min p.i., 1.63 ± 0.42% ID/g 1 h p.i.). Both probes were rapidly excreted through the renal system. The NODA-GA-conjugate showed lower kidney accumulation than the DOTA-conjugate at 1 h p.i. No relevant uptake was observed after 1 h p.i. for both probes.

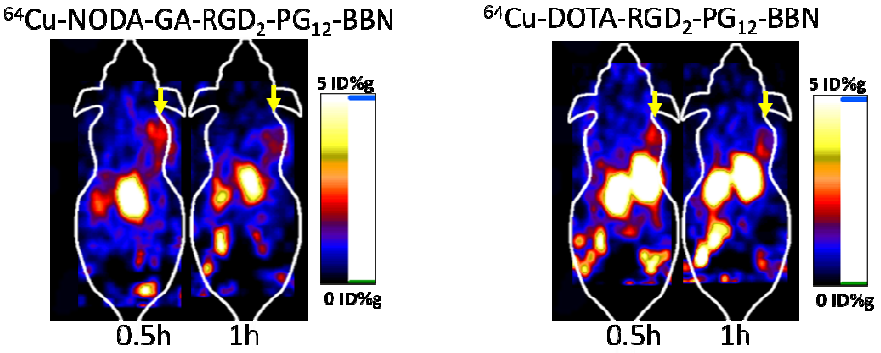

Figure 3. Decay-corrected whole-body coronal microPET images of athymic male nude mice bearing PC-3 tumor on right shoulder from a static scan at 0.5 h and 1 h of ^{64}Cu-DOTA-RGD$_2$-PG$_{12}$-BBN and ^{64}Cu-NODA-GA-RGD$_2$-PG$_{12}$-BBN (100 μCi). Tumors are indicated by arrows.

	organ	30 min (%ID/g)	1h (%ID/g)
^{64}Cu-NODA-GA-RGD$_2$-PG$_{12}$-BBN	Tumor	2.02 ± 0.18	1.80 ± 0.34
	Kidney	7.93 ± 2.19	7.25 ± 1.49
^{64}Cu-DOTA-RGD$_2$-PG$_{12}$-BBN	Tumor	1.92± 0.24	1.63 ± 0.42
	Kidney	7.50 ± 2.80	8.11 ± 3.77

Table 2. MicroPET quantification data of ^{64}Cu-NODA-GA-RGD$_2$-PG$_{12}$-BBN and ^{64}Cu-DOTA-RGD$_2$-PG$_{12}$-BBN.

2) From the coronal microPET images of the mice treated with blocking agents, the tumor was barely visible at all time points (Fig. 4A), including the mice not treated with blocking agents that displayed lower tumor and kidney uptake (1.47±0.12 %ID/g 30 min p.i., 1.16 ±0.18 1h p.i., Table 3). BBN and RGD$_2$ were not able to significantly block the tumor uptake of the probe but only to reduce it, as it is evident from the comparison with the ^{64}Cu-NODA-GA-RGD$_2$-PG$_{12}$-BBN microPET quantification data (Table 2: 2.02 ± 0.18 %ID/g 30 min p.i., 1.80 ± 0.34 %ID/g 60 min p.i.).

Relative low tumor uptake was also observed in the biodistribution study (Fig. 4B). It was found that there is no significant difference for the tumor uptake between non-blocking group and RGD blocking group (P=0.68), BBN blocking (P=0.20), and RGD+BBN blocking group (P=0.63). Also there is no difference for their tumor/muscle ratio between non-blocking group and treated groups (P>0.05) (Fig. S2). Interestingly, it was found that there is significant difference for the tumor-blood ratio between unblocking group and RGD+BBN group (P=0.004). The kidney represents the organ of

major ^{64}Cu-NODA-GA conjugate accumulation, followed by pancreas, stomach, intestine, due to the high BB_2 expression in these organs. The pancreas had predominant uptake of ^{64}Cu-NODA-GA-RGD_2-PG_{12}-BBN at 1 h after injection, which was confirmed by lower pancreatic uptake of the tracer in BBN blocking experiment ($P<0.05$). In the presence of a blocking dose of BBN or RGD plus BBN, the distribution of the probe in lungs, liver and spleen was significantly high.

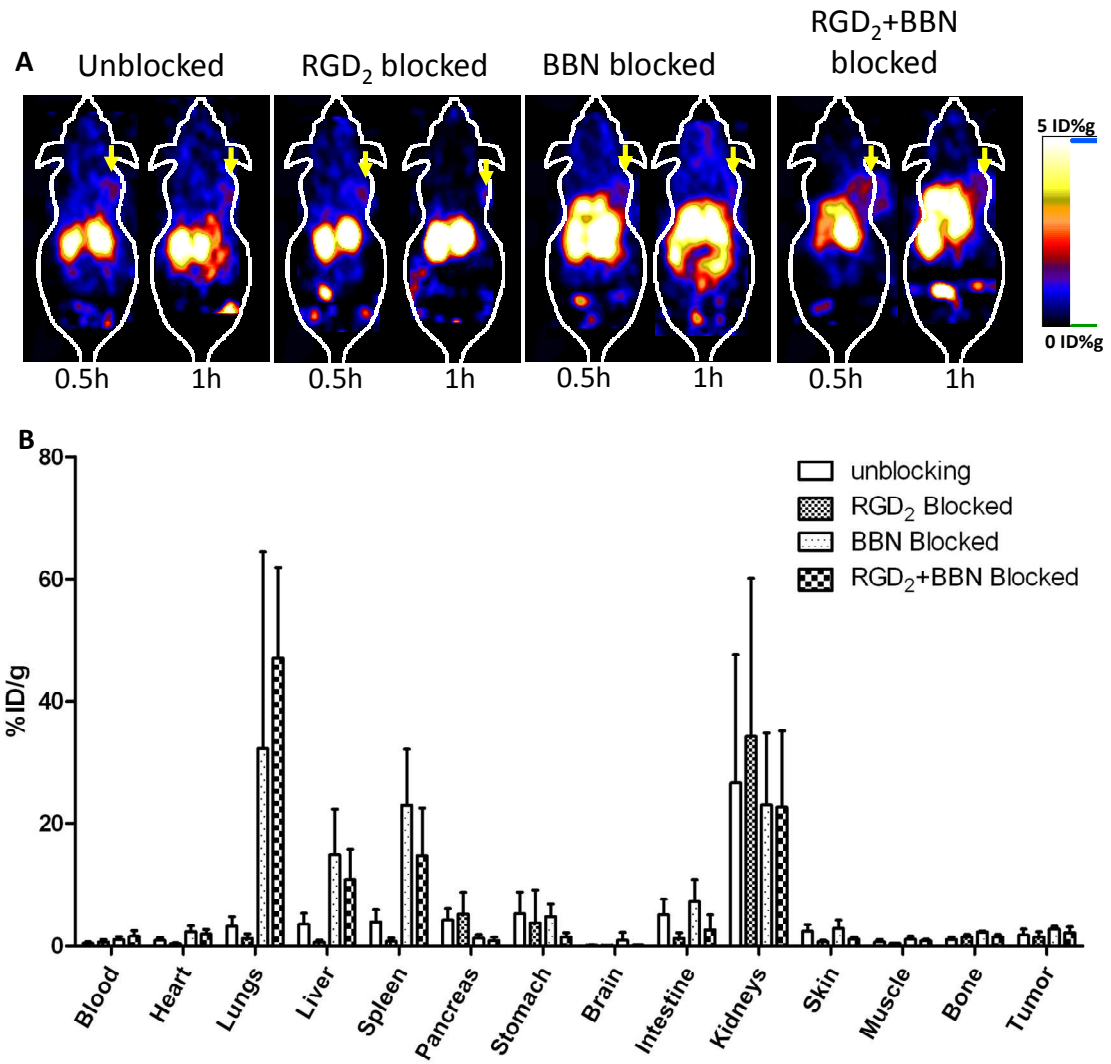

Figure 4. A) Decay-corrected whole-body coronal microPET images of athymic male nude mice bearing PC-3 tumor on right shoulder from a static scan at 0.5 h and 1 h of ^{64}Cu-NODA-GA-RGD_2-PG_{12}-BBN (3.7 MBq, 100μCi) and in the presence of blocking dose of RGD_2, BBN or RGD_2 plus BBN. Tumors are indicated by arrows. B) Biodistribution and blocking studies of ^{64}Cu-NODA-GA-RGD_2-PG_{12}-BBN (3.7 MBq,

100μCi) in athymic male nude mice at 1 h after injection of tracer with or without blocking dose of RGD_2, BBN, or RGD_2 plus BBN.

	organ	30 min (%ID/g)	1h (%ID/g)
Unblocked	Tumor	1.47 ±0.12	1.16 ±0.18
	Kidney	6.38 ± 1.90	5.01 ± 0.21
RGD_2 blocking	Tumor	1.52± 0.12	1.2 ± 0.21
	Kidney	6.59 ± 1.90	5.19 ± 0.06
BBN blocking	Tumor	1.15 ± 0.15	0.9 ± 0.19
	Kidney	4.92 ± 1.13	3.91 ± 0.24
RGD_2+BBN blocking	Tumor	1.20 ± 0.19	0.96 ± 0.26
	Kidney	5.10 ± 1.03	4.06 ± 0.36

Table 3. MicroPET quantification data of ^{64}Cu-NODA-GA-RGD_2-PG_{12}-BBN with or without blocking agents RGD_2, BBN and RGD_2+BBN.

DISCUSSION

The early diagnosis of tumors remains the most important challenge for oncologists, since it is determinant in increasing the chances of cure and reducing the number of deaths.[34] Molecular imaging has displayed a very important role in this field. As PET technology has become more widely available, research efforts have focused on the discovery of new possible biomarkers, on the design of selective ligands and on the development of potential probes, labeled with β^+-emitting isotopes such as ^{11}C, ^{18}F, ^{64}Cu and ^{68}Ga. Since BB_2 and integrin $\alpha_v\beta_3$ receptors are two of the most studied targets for early diagnosis of prostate cancer, RGD-BBN peptide heterodimers, which target both targets, were developed.[13,35,36] The "dual targeting" approach, using RGD-BBN heterodimers, has recently shown significant improvement over BBN or RGD monopeptides as imaging probes. However, their potential application in the clinic is

restricted due to the mixture nature, inefficient synthesis or unfavorable *in vivo* kinetics, which could depend on the linker nature chosen for the RGD-BBN heterodimer design, since they all report short length linkers between the two moieties.[3-10]

Having this goal in mind, it was designed a probe having, between BBN(7-14) and RGD_2 moieties, a long linking chain, that should easily allow the binding of both ligands to their respective receptors. The linker, consisting of PG_{12} chain, was already used to prepare heterobivalent ligands and it showed the highest binding enhancement for the related targets. Furthermore, the PG_{12} linker is easily build directly on the BBN(7-14) moiety through a Fmoc standard solid-phase synthesis.[33] An additional PEG_3 spacer (11-amino-3,6,9-trioxaundecanoic acid) was introduced onto the linker structure, to reduce the heterodimer lipophilicity and to reduce steric hindrance of the molecule.[6,25,37]

^{64}Cu was chosen as radioisotope for RGD_2-BBN heterodimer labeling, due to its numerous favorable decay characteristics (half-life, 12.7 h; β^+, 17.8%; β^- 38.4%) for both diagnostic PET imaging and radiotherapy, compared to the PET isotopes ^{18}F ($t_{1/2}$ = 109.8 mins) and ^{11}C ($t_{1/2}$ = 20.4 mins) currently in use.[10,36,38]

Both DOTA and NODA-GA were introduced as bifunctional chelators for ^{64}Cu labeling. DOTA is one of the most widely studied chelating agent in PET imaging. NODA-GA is a derivative of NOTA, which has the capacity to form more stable complexes with Cu^{2+} and that overcome demetallation and uptake of tracer in hepatic tissue, giving better *in vivo* properties than DOTA.[4,10,39,40] NOTA was modified to obtain the new trifunctional chelator NODA-GA, in order to separate the chelated radiometal, which produces the signal from the peptide, which is the biologically active

entity. In previous studies, NODA-GA showed same radiochemical and biological behaviors than NOTA.[41-43]

In this study, the new ^{64}Cu-labeled probes DOTA- and NODA-GA-RGD_2-PG_{12}-BBN were developed as potential new class of RGD_2-BBN heterotrimer with a long linker structure. In the synthetic phase, the best condition to condense RGD_2-PEG_3 to PG_{12}-BBN involved the use of the coupling agent HATU, in the presence of DIPEA, in DMF. Since the common procedure of DOTA and NODA-GA activation *in situ* failed, or yielded the product in trace, the commercially available DOTA-NHS and NODA-GA-NHS, already activated by the *N*-hydroxysuccinimide group, were directly used for the conjugation to the heterotrimers, with very good yields (Fig. 5). This behaviour could be due to the very poor solubility of DOTA and NOTA acids observed in DMF and DMSO and to the low reactivity of the heterotrimer in the aqueous buffer solutions, required for DOTA and NODA-GA NHS-in situ activation.

The binding assays of DOTA and NODA-GA conjugates were performed on PC-3 and U87MG cells, which express BB_2 and $\alpha_v\beta_3$ receptors, respectively, using the corresponding specific radioligands ^{125}I-[Tyr^4]BBN and ^{125}I-echistatin. Analyzing the IC_{50} values of the probes, it was evident that NODA-GA-RGD_2-PG_{12}-BBN showed better binding affinity (24.3 nM) for BB_2 receptor as compared to other PET RGD-BBN heterodimers reported in literatures from Liu and co-workers (92.75 ± 3.53 nM for NOTA-RGD-BBN, 85.79 ± 2.08 nM for DOTA-RGD-BBN, 73.28 ± 1.57 nM for FB-PEG_3-RGD-BBN, 85.45 ± 1.95 nM for PEG_3-RGD-BBN), Li and co-workers (32.0 ± 1.9 nM for FB-BBN-RDG) and Yan and co-workers (167 ± 1.41 nM for FB-AEADP-BBN-RGD).[3,4,6,7-10,12] NODA-GA-RGD_2-PG_{12}-BBN probe also displayed good affinity

for integrin $\alpha_v\beta_3$ (165.3 nM). DOTA-RGD_2-PG_{12}-BBN still displayed high affinity for BB_2 and $\alpha_v\beta_3$ (100.4 nM and 101.2 respectively). The binding assays proved that the heterotrimers possess dual receptor affinity and that a long linker was beneficial, with NODA-GA probe showing higher BB_2 receptor affinity.

Moreover, NODA-GA probe showed higher ability to complex and retain bivalent metals than DOTA, due to the triazacyclononane cage in common to NOTA and three carboxylate groups available to complex ^{64}Cu (trifunctional chelate system). Radio-HPLC analysis of the probes revealed their stability after 1 h incubation in mouse serum.

^{64}Cu-DOTA- and ^{64}Cu-NODA-GA-RGD_2-PG_{12}-BBN were evaluated *in vivo* in PC-3 tumor model. Both probes rapidly accumulated into the tumor tissue and also showed also high uptake in the kidneys and low in the intestine. The highest uptake into the PC-3 xenografts was evident after 0.5 h p.i. (2.02 ± 0.18 %ID/g for ^{64}Cu-NODA-GA- and 1.92 ± 0.24 %ID/g for ^{64}Cu-DOTA-RGD_2-PG_{12}-BBN), but it was lower compared to the previous heterodimers as FB-RGD-BBN (5.00 ± 0.28 %ID/g)[3], FB-PEG_3-RGD-BBN (6.35 ± 2.52 %ID/g)[6], NOTA-RGD-BBN and DOTA-RGD-BBN, (3.06 ± 0.11 %ID/g and 3.06 ± 0.11 %ID/g respectively)[4] and FB-AEADP-BBN-RGD (5.20 ± 1.04 %ID/g).[8] Radioactivity was still retained in the tumor tissue after 1 h, decreased to 1.80 ± 0.34 %ID/g for ^{64}Cu-NODA-GA- and to 1.63 ± 0.42 %ID/g for ^{64}Cu-DOTA-RGD_2-PG_{12}-BBN, in the same manner as the analog probes. For the NODA-GA conjugate kidney uptake decrease after 0.5 h, unlike the DOTA conjugate that showed an increase in radioactivity after 1 h. These results confirmed NODA-GA

had better kinetics than DOTA, but both probes were rapidly cleared out through the kidneys after 1 h p.i.

Biodistribution studies revealed that 1 h after injection of ^{64}Cu-NODA-GA-RGD_2-PG_{12}-BBN the uptake in the kidneys was predominant and the tumor uptake was low. The statistical analysis indicated that there are no significantly differences for the tumor uptake of non-blocking group and various blocking groups. But significant difference was found for the Tumor/blood ratio between the non-blocking group and RGD+BBN blocking group. Overall, it was not clear if the blocking agents RGD_2 and BBN really prevented the probe accumulation into the tumor considering the overall low uptake.

Lastly, comparing to previous reported RGD-BBN heterodimers with short linker, the probes with long linker reported here show distinctive advantages and disadvantages. The long linker introduced in our probes is able to increase the availability of the two moieties for the BB2 and avb3 receptors, and the resulted DOTA and NODA-GA conjugates demonstrate improved in vitro binding affinities to the targets. But surprisingly, they show low tumor uptakes in vivo, likely attributing to the un-desirable pharmacokinetics and low in vivo stability. This study suggests that further optimization of the RGD-BBN with long linker is required to obtain BB_2 and $\alpha_v\beta_3$ dual targeted PET probe with good in vivo performance. Our study reported here laid down a foundation for design and development of a new class of RGD-BBN long chain dual targeting probe.

CONCLUSION

The aim of the present work was to identify a new dual targeting imaging probe for BB_2 and integrin $\alpha_v\beta_3$ receptors, with an innovative long chain linker, in order to 1) facilitate the preparation, 2) increase the PC-3 tumor affinity and 3) improve the kinetics. 1) NODA-GA- and DOTA-RGD_2-PG_{12}-BBN heterotrimers were successfully prepared and radiolabeled with ^{64}Cu. The radiolabeling yield confirmed the superior radiochemical characteristics of NODA-GA chelator, compared to DOTA. 2) The binding affinity results revealed that the NODA-GA conjugate displayed one of the highest affinity for BB_2 receptor compared to all the other RGD-BBN heterodimers for PET imaging studied to date. Good BB_2 and $\alpha_v\beta_3$ binding affinities were observed for both conjugates, proving the dual targeting ability of the heterotrimers independently from the chelator used. 3) From *in vivo* study, it was observed a low tumor uptake, probably caused by the poor pharmacokinetic properties of the probes. In spite the probes displayed very good *in vitro* properties, they showed suboptimal properties *in vivo* as tracers for PET imaging of tumor tissues overexpressing BB_2 and integrin $\alpha_v\beta_3$-receptors. Nonetheless, the present study represents a step forward the design of effective heterodimer or heterotrimer probes for dual targeting.

EXPERIMENTAL PROCEDURES

General

N-Succinimidyl-1,4,7,10-tetraazacyclododecane-*N*,*N'*,*N''*,*N'''*-tetraacetic acid (DOTA-NHS) and 2,2'-(7-(1-carboxy-4-((2,5-dioxopyrrolidin-1-yl)oxy)-4-oxobutyl)-1,4,7-triazonane-1,4-diyl)diacetic acid (NODA-GA-NHS) were purchased from Macrocyclics Inc (Dallas, TX, United States), and CheMatech (Dijon, France),

respectively. Fmoc-protected amino acids were purchased from Novabiochem/EMD Chemicals Inc (Gibbstown, NJ, United States). Dimethylsulfoxide (DMSO), N,N-dimethylformamide (DMF), diethyl ether, acetonitrile (MeCN), trifluoroacetic acid (TFA), triethylamine, diisopropylcarbodiimide (DIC), piperidine (PIP), N-hydroxybenzotriazole hydrate (HOBt), 2-(1H-7-azabenzotriazol-1-yl)-1,1,3,3-tetramethyl uronium hexafluorophosphate (HATU), N,N-Diisopropylethylamine (DIPEA), ethanedithiole (EDT), triisopropylsilane (TIS), di-tert-butyl dicarbonate (BOC_2O) and all other standard synthesis reagents were purchased from Sigma-Aldrich Chemical Co (Milwaukee, WI, United States). The dimer E[*c*(RGDyK)]$_2$ was obtained from Peptides International (Louisville, KY). All chemicals were of analytical grade and were used without any further purification. The radionuclide, ^{64}Cu was provided by the Department of Medical Physics, University of Wisconsin at Madison. ^{125}I-[Tyr^4]-Bombesin, ^{125}I-Echistatin and the desalting columns (PD-10) were purchased from GE healthcare (Piscataway, NJ). The syringe filter and polyethersulfone membranes (pore size, 0.22 μm; diameter, 13 mm) were obtained from Nalge Nunc International (Rochester, NY). The semi-preparative reversed-phase high-performance liquid chromatography (HPLC) was performed on a Dionex 680 chromatography system equipped with a Vydac protein and peptide column (218TP510; 5μm, 250 × 10 mm) and with a UVD 170U absorbance detector (Sunnyvale, CA) and model 105S single-channel radiation detector (Carroll & Ramsey Associates). The UV absorbance was monitored at 218 nm and the identification of the peptides was confirmed on the basis of UV spectrum, acquired using a photodiode array (PDA) detector. The mobile phase was composed by the solvent A, 0.1% TFA in water, and the solvent B, 0.1% TFA in MeCN,

with a flow rate of 3 or 4 mL/min. Analytical HPLC was performed with a Vydac protein and peptide column (218TP510; 5 μm, 250 × 4.6 mm). The recorded data were processed using Chromeleon version 6.50 software. Peptide purity and molecular mass were determined by analytical scale RP-HPLC and matrix-assisted laser desorption/ionization time of flight mass spectrometry (MALDI-TOF-MS).

Synthesis of E-PG$_{12}$-BBN

H-Glu-(Pro-Gly)$_{12}$-BBN(7-14)-NH$_2$ [H-E-(P-G)$_{12}$-Q-W-A-V-G-H-L-M-NH$_2$] (**2**, E-PG$_{12}$-BBN) was obtained using standard Fmoc solid-phase peptide synthesis method on an automated peptide synthesizer (CS Bio, CS 336X). Briefly, Rink Amide LS resin (200 mg, 40 μmol, Advanced ChemTech, 0.2 mmol/g loading) was swollen in DMF for 30 min. Fmoc groups were removed with 20% PIP in DMF. The aliquots of amino acids (0.50 mmol) were activated in a solution containing 0.50 mmol of HOBt and 0.5 M DIC in DMF. Peptide cleavage and deprotection were carried out by 3 h incubation in a mixture of TFA/TIS/EDT/H_2O (94:2:2:2). The mixture was filtered, the peptide in solution was precipitated with cold anhydrous diethyl ether and centrifuged. The resulting peptide was dissolved in water and purified by RP-HPLC, with a mobile phase gradient from 80% solvent A and 20% B (0-2 min) to 55% solvent A and 45% solvent B at 32 min, with a flow rate of 4 mL/min. Fractions were collected, evaporated *in vacuo* and lyophilized. The target product was characterized by the MALDI-TOF-MS and ready for use in the next step reaction. Analytical HPLC (t_R = 18.1 min) and MALDI-TOF-MS: m/z 2918.3 for $[M]^+$, 1460.1 for $[M+2H]^{2+}$ (Chemical Formula: $C_{133}H_{193}N_{37}O_{36}S$, calculated molecular weight 2918.2).

Synthesis of RGD_2-PG_{12}-BBN heterotrimer

The peptide E-PG_{12}-BBN (**2**, 1 eq) was protected with $(Boc)_2O$ (50 eq) on the N-terminus in 500 μL of DMF and 10 μL of Et_3N at room temperature overnight. Then the product was purified on the semi-preparative RP-HPLC, with a mobile phase gradient from 75% solvent A and 25% B (0-2 min) to 55% solvent A and 45% solvent B at 32 min, with a flow rate of 3 mL/min. The solvent was removed by evaporation *in vacuo* and lyophilization to give a fluffy white powder. Yield: 65%. Analytical HPLC (t_R = 19.7 min). MALDI-TOF-MS: m/z 3017.9 for $[M]^+$ (Chemical Formula: $C_{138}H_{201}N_{37}O_{38}S$, calculated molecular weight 3018.4).

The Boc-protected peptide (**3**, 1 eq) was added to a solution of HATU (1.5 eq) and DIPEA (3 eq) in 500 μL of DMF and the reaction mixture was vortexed at room temperature for 2 hours. Then E[*c*(RGDyK)]$_2$-PEG_3 (RGD_2-PEG_3) (1.5 eq) was added to the solution of the peptide, activated on the Glu side chain, and stirred overnight at room temperature. The semi-preparative RP-HPLC was used for the purification, from 75% solvent A and 25% B (0-2 min) to 45% solvent A and 55% solvent B at 32 min, with a flow rate of 3 mL/min. Fractions were collected, evaporated *in vacuo* and lyophilized. Yield: 36%. Analytical HPLC (t_R = 19.3 min). MALDI-TOF-MS: m/z 4539.7 for $[M]^+$ (Chemical Formula: $C_{205}H_{301}N_{57}O_{59}S$, calculated molecular weight 4540.0).

The Boc-protected heterotrimer RGD_2-PEG_3-Glu-$(Pro\text{-}Gly)_{12}$-BBN(7-14)-NH_2 (**4**) was deprotected with TFA in MeCN for 30 min, at room temperature and the product was isolated by semipreparative HPLC from 80% solvent A and 20% B (0-2 min) to 35% solvent A and 65% solvent B at 32 min, with a flow rate of 3 mL/min. The

collected fractions were combined, evaporated *in vacuo* and lyophilized to afford the final product E[*c*(RGDyK)]$_2$-PEG$_3$-Glu-(Pro-Gly)$_{12}$-BBN(7-14)-NH$_2$ (**5**, named as RGD$_2$-PG$_{12}$-BBN), as a white powder. Yield: 60%. Analytical HPLC (t_R = 18.3 min). MALDI-TOF-MS: m/z 4439.6 for $[M]^+$, 2220.8 for $[M+2H]^{2+}$ (Chemical Formula: $C_{200}H_{293}N_{57}O_{57}S$, calculated molecular weight 4439.9).

Synthesis of DOTA and NODA-GA conjugates

A solution of RGD$_2$-PG$_{12}$-BBN (1 eq) was mixed with DOTA-NHS (50 eq) and stirred for 1 hour at room temperature in DMF and DIPEA. The DOTA conjugate was isolated by semipreparative HPLC from 80% solvent A and 20% B (0-2 min) to 45% solvent A and 55% solvent B at 32 min, with a flow rate of 3 mL/min The collected fractions were combined, evaporated *in vacuo* and lyophilized to afford the final product DOTA-RGD$_2$-PG$_{12}$-BBN (**6**) as a white powder (Fig. 5). Yield: 99%. Analytical HPLC (t_R = 18.1 min). MALDI-TOF-MS: m/z 4826.1 for $[M]^+$ (Chemical Formula: $C_{216}H_{319}N_{61}O_{64}S$, calculated molecular weight 4826.3). The same procedure was used to obtain NODA-GA-RGD$_2$-PG$_{12}$-BBN, from RGD$_2$-PG$_{12}$-BBN (1 eq) and NODA-GA-NHS (3 eq) (**7**) (Fig. 5). Yield: 78%. Analytical HPLC (t_R = 18.3 min). MALDI-TOF-MS: m/z 4799.0 for $[M+H]^+$, 2399.9 for $[M+2H]^{2+}$ (Chemical Formula: $C_{215}H_{316}N_{60}O_{64}S$, calculated molecular weight 4797.2). (Fig. 3)

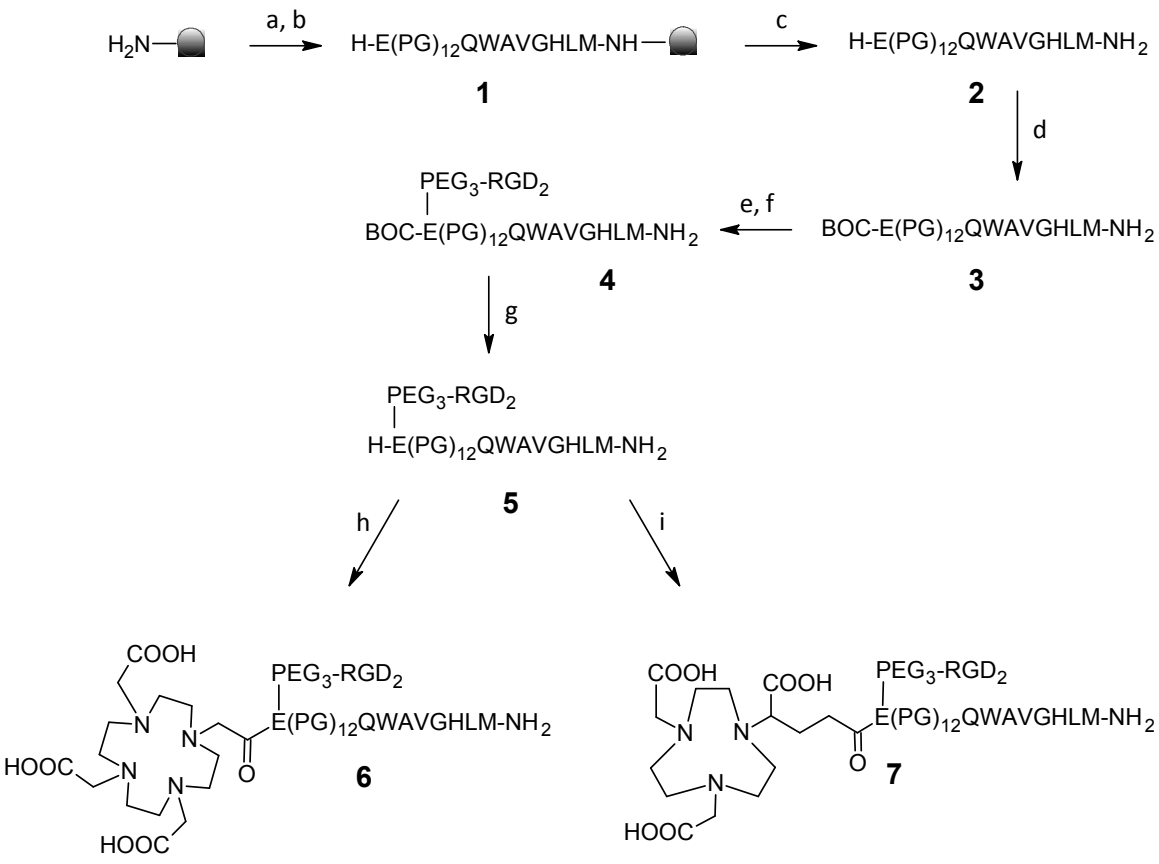

Figure 5. NODA-GA-RGD_2-PG_{12}-BBN and DOTA-RGD_2-PG_{12}-BBN solid phase and in solution synthesis.
a) Fmoc-AA-OH, HOBt, DIC; b) PIP 20% in DMF; c) TFA-scavengers cocktail, 2h, r.t.; d) $(BOC)_2O$, Et_3N in DMF, o.n., r.t.; e) HATU, DIPEA in DMF, 2h, r.t.; f) RGD_2-PEG_3, o.n., r.t.; g) TFA in MeCN, 30 min, r.t.; h) DOTA-NHS, DIPEA in DMF, 1h, r.t. i) NODA-GA-NHS, DIPEA in DMF, 1h, r.t.

^{64}Cu radiolabeling of DOTA-RGD_2-BBN and NODA-GA-RGD_2-BBN heterotrimers

The conjugates DOTA-RGD_2-PG_{12}-BBN and NODA-GA-RGD_2-PG_{12}-BBN (5-10 nmol) were radiolabeled with ^{64}Cu by addition of $^{64}CuCl_2$ (88.8 MBq, 2.4 mCi) in 0.1 N sodium acetate buffer (NaOAc, pH 6) at 42 °C. The NODA-GA-peptide complexed with ^{64}Cu in 15 minutes with the yield of 70%; it showed better radiolabeling ability than DOTA-peptide, that was able to complex the radioisotope in 1 h with the

yield of 40%. The radiolabeled complexes were purified by PD-10 columns, washed out by phosphate-buffered saline (PBS, pH 7.4, 0.01M) and passed through a 0.22-μm Millipore filter into a sterile vial for *in vitro* and *in vivo* experiments. Radioanalytical HPLC was used to analyze the purified ^{64}Cu-DOTA-RGD$_2$-PG$_{12}$-BBN (**8**) and ^{64}Cu-NODA-GA-RGD$_2$-PG$_{12}$-BBN (**9**).

Mouse Serum Stability

^{64}Cu-DOTA-RGD$_2$-PG$_{12}$-BBN and ^{64}Cu-NODA-GA-RGD$_2$-PG$_{12}$-BBN (7.4-11.1 MBq, 200-300 μCi) in 500 μL of PBS were added to 500 μL of mouse serum (Sigma). After incubation at 37 °C for 1 h, the incubation mixtures (100 μL, 1.48-2.22 MBq, 40-60 μCi) were precipitated with 10% of MeCN and centrifuged through a Spin-X centrifuge tube filter (pore size 0.22 μm, diameter 13 mm, COSTAR). The supernatants were then injected into the radio-HPLC under the same conditions used for analyzing ^{64}Cu-DOTA-RGD$_2$-PG$_{12}$-BBN and ^{64}Cu-NODA-GA-RGD$_2$-PG$_{12}$-BBN radiolabeling reactions.

Cell Culture and Animal Models

The PC-3 human prostate carcinoma cell line and the U87MG human glioblastoma cell line were purchased from American Type Culture Collection (ATCC, Manassas, VA). PC-3 cells were grown in RMPI 1640 medium (Invitrogen) supplemented with 10% (v/v) fetal bovine serum (FBS, Invitrogen) and 1% penicillin-streptomycin. U87MG cells were cultured in DMEM containing high glucose (GIBCO, Carlsbad, CA), which was supplemented with 10% FBS and 1% penicillin-

streptomycin. The cells were expanded in tissue culture dishes and kept in a humidified atmosphere of 5% CO_2 at 37 °C. The medium was changed every other day. A confluent monolayer was detached with 0.05% Trypsin in 0.01M PBS (pH 7.4) and dissociated into a single-cell suspension for further cell culture. Animal procedures were performed according to a protocol approved by the Stanford University Institutional Animal Care and Use Committee. Approximately 3×10^6 cultured PC-3 cells were suspended in PBS and subcutaneously implanted in the right shoulders of male nude mice purchased from Charles River Laboratory (Wilmington, MA). Tumors were allowed to grow to a size of 0.5-1 cm in diameter (3~4 weeks).

PC-3 and U87MG Binding assay

The *in vitro* BB_2 binding affinity of DOTA- and NODA-GA-RGD_2-PG_{12}-BBN conjugates were determined by competitive displacement of ^{125}I-[Tyr^4]BBN, as BB_2-specific radioligand, on PC-3 cell line. Briefly, PC-3 cells (5×10^6) were suspended in the binding buffer (RPMI 1640 medium supplemented with 2 mg/mL bovine serum albumin (BSA) and 5.2 mg/mL HEPES), then seeded in Millipore 96-well filter multiscreen DV plates (pore size 0.65 μm), previously filled with increasing concentration of the appropriate conjugate (10^{-12} to 10^{-6} M) and ^{125}I-[Tyr^4]BBN. After incubation for 1 h at 37 °C, the cells were washed three times with chilled PBS, filtered through a multiscreen vacuum manifold to remove any unbound radioligand. The filters at the well bottoms were dried and collected to measure the filter-bound radioactivity, by means of a γ-counter (PerkinElmer 1470, Waltham, MA). The data were plotted in GraphPad Prism (GraphPad Software, Inc., San Diego, CA, USA) to elaborate the

binding sigmoid curves and to obtain the half maximal inhibitory concentration (IC_{50}). Experiments were run in triplicate.

Similarly, *in vitro* integrin $\alpha_v\beta_3$ binding affinity of DOTA- and NODA-GA-RGD_2-PG_{12}-BBN was assessed on U87MG $\alpha_v\beta_3$ positive cells using ^{125}I-echistatin as specific radioligand. The cells (6×10^6) were incubated in Millipore 96-well filter multiscreen DV plates (pore size 0.65 μm) with ^{125}I-echistatin and (at various concentrations) the test compounds (DOTA- or NODA-GA-RGD_2-PG_{12}-BBN) in the binding buffer (IBB, 25 mM Tris pH 7.4, 150 mM NaCl, 2 mM $CaCl_2$, 1 mM $MgCl_2$, 1 mM $MnCl_2$, and 0.1% BSA) at 37 °C for 1 h. Experiments were performed in triplicate and IC_{50} values were determined as described above.

Small-Animal PET Imaging

Small animal PET imaging of PC-3 tumor-bearing mice was performed on a microPET R4 rodent model scanner (Siemens Medical Solutions USA, Inc.) as previously-reported.[3] Mice (n = 3-4 for each group) were anesthetized with isoflurane (5% for induction and 2% for maintenance in 100% O_2) before injection and scan times. ^{64}Cu-DOTA-RGD_2-BBN or ^{64}Cu-NODA-GA-RGD_2-BBN (3.15-3.52 MBq, 85-95 μCi) were injected *via* the tail vein, and, at 0.5 h and 1 h p.i., the mice were placed in the prone position, near the center of the microPET field of view (FOV), for the 3-min static scans acquisition. The ^{64}Cu-NODA-GA-RGD_2-PG_{12}-BBN blocking studies (n = 3) were performed by co-injection of this probe (3.7 MBq, 100 μCi) with RGD_2 and/or BBN (200 μg respectively), followed 3-min static microPET images acquisition at 0.5 h and 1 h, as reported.[4]

Biodistribution Studies of ^{64}Cu-NODA-GA-RGD$_2$-PG$_{12}$-BBN

For biodistribution studies, nude mice (n = 3 for each group), bearing PC-3 xenografts, were injected with 3.7 MBq (100 μCi) of ^{64}Cu-NODA-GA-RGD$_2$-PG$_{12}$-BBN *via* the tail vein and saturating doses of RGD$_2$ and/or BBN (200 μg respectively) were co-injected (with the probe) for the blocking studies. Then, the mice were sacrificed at 1 h p.i. Tumor and other organs of interest were collected, weighed, and their radioactivity was measured in a γ-counter. The results were expressed as a percentage of the injected radioactive dose per gram of tissue (% ID/g).[4]

Statistical Methods

Statistical analysis was performed using the Student's two-tail *t*-test for unpaired data. A 95% confidence level was chosen to determine the significance between groups, with $P < 0.05$ being significantly different.

ACKNOWLEDGEMENTS

We acknowledge the support from the DOD-PCRP-NIA PC094646 (ZC), the fellowship from ADISU Agency, for financing part of E. Lucente stay at Stanford University, and the National Basic Research Program of China (2015CB931800). We thank Kai Cheng and Kenneth Lau for carrying out the MALDI-TOF-MS analysis, Yingding Xu and Han Jiang for their support in biological studies, Jinbo Li, Song Wu and Shibo Qi for the help in HPLC analysis and solid phase synthesis.

Supporting Information:

This material is available free of charge via the Internet at http://pubs.acs.org.

Corresponding Author Information

Zhen Cheng, Ph.D., Molecular Imaging Program at Stanford, Department of Radiology and Bio-X Program, Canary Center at Stanford for Cancer Early Detection, 1201 Welch Road, Lucas Expansion, P095, Stanford University, Stanford, CA 94305, USA. E-mail: zcheng@stanford.edu; Phone: +1 650 7237866; Fax +1 650 7367925

Marcello Leopoldo, Dipartimento di Farmacia – Scienze del Farmaco, Università degli Studi di Bari Aldo Moro, via Orabona, 4, 70125, Bari, Italy. E-mail: marcello.leopoldo@uniba.it; Phone: +39 080 5442798; Fax: +39 080 5442231.

ORCID:

Zhen Cheng: 0000-0001-8177-9463

Marcello Leopoldo: 0000-0001-8401-2815

Notes
The authors declare no competing financial interest.

ABBREVIATIONS

BBN: bombesin;

RGD_2: cyclic arginine-glycine-aspartic acid dimer peptide;

GRPR: gastrin-releasing peptide receptor;

DOTA: 1,4,7,10-tetraazacyclododecane-1,4,7,10-tetraacetic acid;

NODA-GA: 1,4,7-triazacyclononane-1-glutaric acid-4,7-diacetic acid;

PET: positron emission tomography;

p.i.: postinjection.

REFERENCES

1. Yan, Y., and Chen, X. (2011) Peptide heterodimers for molecular imaging. *Amino Acids*. *41,* 1081-1092.
2. Reubi, J. C., and Waser, B. (2003) Concomitant expression of several peptide receptors in neuroendocrine tumours: Molecular basis for in vivo multireceptor tumour targeting. *Eur J Nucl Med Mol Imaging*. *30,* 781–793.
3. Li, Z. B., Wu, Z., Chen, K., Ryu, E. K., and Chen, X. (2008) ^{18}F-labeled BBN-RGD heterodimer for Prostate Cancer Imaging. *J Nucl Med. 49,* 453–461.
4. Liu, Z., Li, Z. B., Cao, Q., Liu, S., Wang, F., and Chen, X. (2009) Small-Animal PET of tumors with ^{64}Cu-Labeled RGD-Bombesin heterodimer. *J Nucl Med. 50,* 1168–1177.
5. Liu, Z., Niu, G., Wang, F., and Chen, X. (2009) ^{68}Ga-labeled NOTA-RGD-BBN peptide for dual integrin and GRPR-targeted tumor imaging. *Eur J Nucl Med Mol Imaging. 36,* 1483–1494.
6. Liu, Z., Yan, Y., Chin, F. T., Wang, F., and Chen, X. (2009) Dual integrin and gastrin-releasing peptide receptor targeted tumor imaging using ^{18}F-labeled PEGylated RGD-Bombesin heterodimer ^{18}F-FB-PEG$_3$-Glu-RGD-BBN. *J Med Chem*. *52,* 425–432.
7. Liu, Z., Yan, Y., Liu, S., Wang, F., and Chen, X. (2009) ^{18}F, ^{64}Cu, and ^{68}Ga labeled RGD-bombesin heterodimeric peptides for PET imaging of breast cancer. *Bioconjug Chem. 20,* 1016–1025

8. Yan, Y., Chen, K., Yang, M., Sun, X., Liu, S., and Chen, X. (2011) A new ^{18}F-labeled BBN-RGD peptide heterodimer with a symmetric linker for prostate cancer imaging. *Amino Acids. 4,* 439-447.

9. Ma, M. T., and Donnelly, P. S. (2011) Peptide targeted copper-64 radiopharmaceuticals. *Curr. Top. Med. Chem. 11,* 500-520.

10. Jackson, A. B., Nanda, P. K., Rold, T. L., Sieckman, G. L., Szczodroski, A. F., Hoffman, T. J., Chen X., and Smith C. J. (2012) ^{64}Cu-NO2A-RGD-Glu-6-Ahx-BBN(7-14)NH_2: a heterodimeric targeting vector for positron emission tomography imaging of prostate cancer. *Nucl Med Biol. 39*, 377-387.

11. Zhang, J., Niu, G., Lang, L., Li, F., Fan, X., Yan, X., Yao, S., Yan, W., Huo, L., Chen, L., et al. (2016) Clinical translation of a dual integrin $\alpha_v\beta_3$ and GRPR targeting PET radiotracer ^{68}Ga-NOTA-BBN-RGD. *J Nucl Med. 58,* 228–234.

12. Sancho, V., Di Florio A., Moody T. W., and Jensen R. T. (2011) Bombesin receptor-mediated imaging and cytotoxicity: review and current status. *Curr. Drug. Deliv. 8,* 79-134.

13. Jensen, R. T., Battey, J. F., Spindel, E. R., and Benya, R. V. (2008) International Union of Pharmacology. LXVIII. Mammalian bombesin receptors: nomenclature, distribution, pharmacology, signaling, and functions in normal and disease states. *Pharmacol Rev. 60,* 1-42.

14. Jensen, R. T., and Moody, T. W. (2006) Bombesin-related peptides and neurotensin: effects on cancer growth/proliferation and cellular signaling in cancer. *Handbook of Biologically Active Peptides*, 429-434.

15. Patel, O., Shulkes, A., and Baldwin, G. S. (2006) Gastrin-releasing peptide and cancer. *Biochim Biophys Acta. 1766,* 23–41.

16. Parry, J. J., Andrews, R., and Rogers, B. E. (2007) MicroPET imaging of breast cancer using radiolabeled bombesin analogs targeting the gastrin-releasing peptide receptor. *Breast Cancer Res Treat. 18,* 110–117.

17. Dimitrakopoulou-Strauss, A., Hohenberger, P., Haberkorn, U., Macke, H. R., Eisenhut, M., and Strauss, L. G. (2007) ^{68}Ga-Labeled bombesin studies in patients

with gastrointestinal stromal tumors: comparison with ^{18}FFDG. *J Nucl Med*. *48,* 1245–1250.

18. Plonowski, A., Nagy, A., Schally, A. V., Sun, B., Groot, K., and Halmos, G. (2000) In vivo inhibition of PC-3 human androgen-independent prostate cancer by a targeted cytotoxic bombesin analogue, AN-215. *Int J Cancer. 88,* 652–657.

19. Smith, C. J., Volkert, W. A., and Hoffman, T. J. (2003) Gastrin releasing peptide (GRP) receptor targeted radiopharmaceuticals: a concise update. *Nucl Med Biol. 30,* 861–868.

20. Smith, C. J., Volkert, W. A., and Hoffman, T. J. (2005) Radiolabeled peptide conjugates for targeting of the bombesin receptor superfamily subtypes. *Nucl Med Biol*. *32,* 733–40.

21. Brooks, P. C., Clark, R. A., and Cheresh, D. A. (1994) Requirement of vascular integrin $\alpha_v\beta_3$ for angiogenesis. *Science*. *264*, 569-571.

22. Kumar, C. C. (2003) Integrin $\alpha_v\beta_3$ as a therapeutic target for blocking tumor-induced angiogenesis. *Curr. Drug Targets*. *4,* 123-131.

23. Hood, J. D., and Cheresh D. A. (2002) Role of integrins in cell invasion and migration. *Nat. Rev. Cancer. 2,* 91-100.

24. Jin, H., and Varner, J. (2004) Integrins: roles in cancer development and as treatment targets. *Br. J. Cancer*. *90*, 561-565.

25. Cai, W., Gambhir, S. S., and Chen, X. (2005) Multimodality tumor imaging targeting integrin $\alpha_v\beta_3$. *BioTechniques. 39,* 14-25.

26. Ruoslahti, E. (1996) RGD and other recognition sequences for integrins. *Annu. Rev. Cell Dev. Biol. 12*, 697-715.

27. Chen, X., Liu S., Hou, Y., Tohme, M., Park, R., Bading, R., and Conti P. S. (2004) MicroPET imaging of breast cancer $\alpha_v\beta_3$-integrin expression with ^{64}Cu-labeled dimeric RGD peptides. *Mol. Imaging Biol*. *6*, 350-359.

28. Chen, X., Tohme, M., Park, R., Hou, Y., Bading, J. R., and Conti P. S. (2004) Micro-PET imaging of $\alpha_v\beta_3$-integrin expression with ^{18}F-labeled dimeric RGD peptide. *Mol. Imaging 3,* 96-104.

29. Chen, X., Hou, Y., Tohme, M., Park, R., Khankaldyyan, V., Gonzales-Gomez, I., Bading, J. R., Laug, W. E., and Conti, P. S. (2004) Pegylated Arg-Gly-Asp peptide: ^{64}Cu labeling and PET imaging of brain tumor $\alpha_v\beta_3$-integrin expression. *J. Nucl. Med. 45*, 1776-1783.

30. Chen, X., Sievers, E., Hou, Y., Park, R., Tohme, M., Bart, R., Bremner, R., Bading, J. R., and Conti P. S. (2005) Integrin $\alpha_v\beta_3$-targeted imaging of lung cancer. *Neoplasia*. *7,* 271-279.

31. Cui, L., Liu, Z., Jin, X., Jia, B., Li, F., and Wang, F. (2013) Evaluation of ^{188}Re-MAG_2-RGD-bombesin for potential prostate cancer therapy. *Nucl Med Biol. 40*, 182-189.

32. Jiang, L., Miao, Z., Liu, H., Ren, G., Bao, A., Cutler, C. S., Shi, H., and Cheng, Z. ^{177}Lu-labeled RGD-BBN heterodimeric peptide for targeting prostate carcinoma. (2013) *Nucl Med Commun*. *34,* 909-914.

33. Vagner, J., Xu, L., Handl, H. L., Josan, J. S., Morse, D. L., Mash, E. A., Gillies, R. J., and Hruby, V. J. (2008) Heterobivalent ligands crosslink multiple cell-surface receptors: the human melanocortin-4 and deltaopioid receptors. *Angew. Chem. Int. Ed. Engl. 47,* 1685-1688.

34. Reubi, C. R. (2003) Peptide receptors as molecular targets for cancer diagnosis and therapy. *Endocr. Rev. 24,* 389-427.

35. Markwalder, R., and Reubi, J. C. (1999) Gastrin releasing peptide receptors in the human prostate: relation to neoplastic transformation. *Cancer Res*. *59,* 1152-1159.

36. Ananias, H. J., de Jong, I. J., Dierckx, R. A., van de Wiele, C., Helfrich, W., and Elsinga, P. H. (2008) Nuclear imaging of prostate cancer with gastrin-releasing-peptide-receptor targeted radiopharmaceuticals. *Curr. Pharm. Des. 14,* 3033-3047

37. Wu, Z., Li, Z. B., Cai, W., He, L., Chin, F. T., Li, F., and Chen, X. (2007) ^{18}F labeled mini-PEG spacered RGD dimer (^{18}F-FPRGD2): synthesis and microPET imaging of $\alpha_v\beta_3$ integrin expression. *Eur. J. Nucl. Med. Mol. Imaging*. *34*, 1823-1831.

38. Wadas, T. J., Wong, E. H., Weisman, G. R., and Anderson, C. J. (2007) Copper chelation chemistry and its role in copper radiopharmaceuticals. *Curr. Pharm. Des. 13*, 3-16.

39. Ait-Mohand, S., Fournier, P., Dumulon-Perreault, V., Kiefer, G. E., Jurek, P., Ferreira, C. L., Bénard, F., and Guérin, B. (2011) Evaluation of ^{64}Cu-labeled bifunctional chelate-bombesin conjugates. *Bioconjug Chem. 22,* 1729-1735.

40. Prasanphanich, A. F., Nanda, P. K., Rold, T. L., Ma, L., Lewis, M. R., Garrison, J. C., Hoffman, T. J., Sieckman, G. L., Figueroa, S. D., and Smith, C. J. (2007) ^{64}Cu-NOTA-8-Aoc-BBN(7-14)NH_2] targeting vector for positron-emission tomography imaging of gastrin-releasing peptide receptor-expressing tissues. *Proc. Natl. Acad. Sci. U. S. A. 104,* 12462-12467.

41. Knetsch, P. A., Petrik, M., Griessinger, C. M., Rangger, C., Fani, M., Kesenheimer, C., von Guggenberg, E., Pichler, B. J., Virgolini, I., Decristoforo, C., et al. (2011) [^{68}Ga]NODAGA-RGD for imaging $\alpha_v\beta_3$ integrin expression. *Eur J Nucl Med Mol Imaging. 38,* 1303-1312.

42. Maecke, H. R. (2005) Radiolabeled peptides in nuclear oncology: influence of peptide structure and labeling strategy on pharmacology. *Ernst. Schering Res. FoundWorkshop. 49,* 43-72.

43. Fani, M., Del Pozzo, L., Abiraj, K., Mansi, R., Tamma, M. L., Cescato, R., Waser, B., Weber, W. A., Reubi, J. C., and Maecke, H. R. (2011) PET of somatostatin receptor-positive tumors using ^{64}Cu- and ^{68}Ga-somatostatin antagonists: the chelate makes the difference. *J Nucl Med. 52,* 1110-1118.

Table of Contents Graphic